ChemComm

Stabilization of bicelles using metal-binding peptide for extended blood circulation

Journal:	*ChemComm*
Manuscript ID	CC-COM-02-2022-001058.R1
Article Type:	Communication

COMMUNICATION

Stabilization of bicelles using metal-binding peptide for extended blood circulation

Yuichiro Takagi,[a] Noriyuki Uchida,*[a] Yasutaka Anraku,[bc] and Takahiro Muraoka*[ade]

Received 00th January 20xx,
Accepted 00th January 20xx

DOI: 10.1039/x0xx00000x

A metal-binding peptide appending cholic acid, Chol-MBP, formed bicelles by mixing with 1,2-dipalmitoyl-*sn*-glycero-3-phosphorylcholine (DPPC). Coordination of Chol-MBP with Cu^{2+} stabilized DPPC bicelles against dilution and contamination of serum proteins, enabling extended blood circulation. This study demonstrates an effective supramolecular design of phospholipid bicelles with enhanced stability useful for membrane-based biomaterials.

Phospholipid-based self-assemblies, such as liposomes have been widely used as biomaterials taking advantage of their biocompatibility because of their similarity to the cell membranes.[1] Bicelles, disk-shaped phospholipid supramolecular assemblies whose edge is stabilized by specific surfactants, have recently attracted much attention due to the characteristic functions derived from the two-dimensional shape.[2] For example, magnetically orientable bicelles have been actively used as alignment media to orient biomolecules in solution for nuclear magnetic resonance (NMR) studies.[2d–2g] More recently, bicelles have also been used as transdermal drug delivery systems because they can pass through narrow gaps between cells in the stratum corneum allowing for efficient penetrations into the skin tissue.[2h] Furthermore, disk-shaped polymer colloids are known to show longer blood circulation[2i] and stronger adhesion to microvascular networks[2j,2k] than spherical colloids, making the disk-shaped materials potentially useful for blood administration.[2l] However, bicelles constructed by supramolecular assemblies of phospholipids and surfactants are generally unstable, and the surfactants are often cytotoxic.[2o] Bicelles consisting of polymerizable siloxane-appended lipids for the stabilization of the disk structures have been reported.[2l–2n] However, the covalent cross-linking of bilayer would largely change fluidity and surface properties of the membrane and decrease biodegradability compared to phospholipid bilayers. Thus, it is still challenging to design structurally stable bicelles consisting of more biocompatible molecules through non-covalent bonding. Nanodiscs whose edges are stabilized by amphiphilic macromolecules[3] have been developed, although their applications to *in vivo* delivery have not been well explored. Blood is a crowding environment containing serum proteins, and nano-objects injected into blood vessels are diluted by the blood circulation. Due to the low physical stability of conventional phospholipid-based bicelles under such physiological conditions, the comparison of blood circulation profiles between disk-shaped bicelles and spherical liposomes[4] has not yet been investigated.

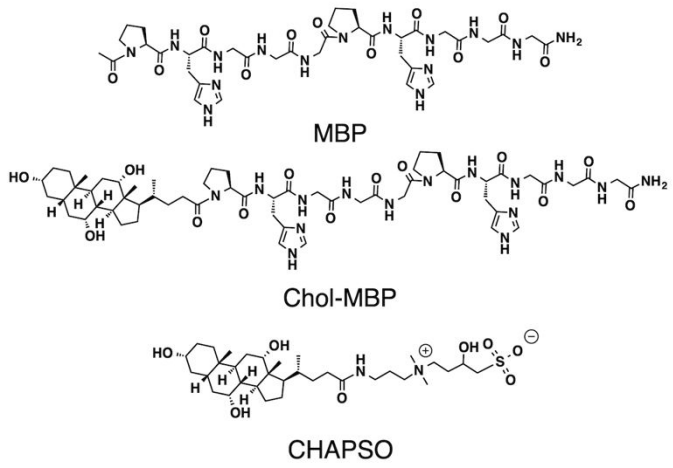

Fig. 1 Molecular structures of MBP, Chol-MBP, and CHAPSO.

Bicelles can be prepared by mixing phospholipids with surfactants that are localized at the edge of the bilayer membranes to inhibit their fusion. For example, 3-[(3-cholamidopropyl)dimethylammonio]-2-hydroxy-1-propanesulfonate (CHAPSO; Fig. 1) can be used as the

[a] *Department of Applied Chemistry, Graduate School of Engineering, Tokyo University of Agriculture and Technology, 2-24-16 Naka-cho, Koganei, Tokyo 184-8588, Japan.*
[b] *Department of Bioengineering, Graduate School of Engineering The University of Tokyo7-3-1 Hongo, Bunkyo-ku, Tokyo 113-8656, Japan.*
[c] *Innovation Center of Nanomedicine Kawasaki Institute of Industrial Promotion3-25-14, Tonomachi, Kawasaki-ku, Kawasaki 210-0821, Japan.*
[d] *Institute of Global Innovation Research, Tokyo University of Agriculture and Technology, 3-8-1 Harumi-cho, Fuchu-shi, Tokyo 183-8538, Japan.*
[e] *Kanagawa Institute of Industrial Science and Technology (KISTEC), 705-1 Shimoimaizumi, Ebina, Kanagawa 243-0435, Japan.*
† Footnotes relating to the title and/or authors should appear here.
Electronic Supplementary Information (ESI) available: Materials, instruments, sample preparation, synthesis, and figures. See DOI: 10.1039/x0xx00000x

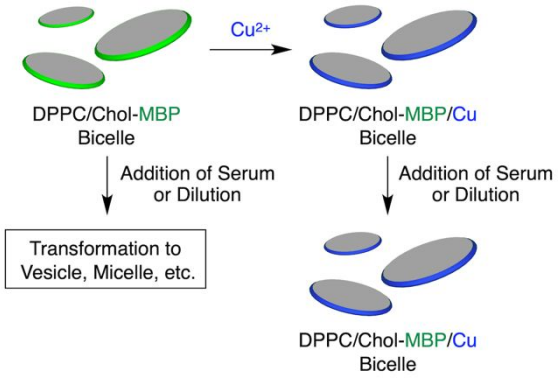

Fig. 2 Schematic illustration of the preparation of DPPC/Chol-MBP bicelles and subsequent Cu^{2+}-medicated metal coordination at Chol-MBP affording crosslinked DPPC/Chol-MBP/Cu bicelles. After the crosslinking, the disk structure of DPPC/Chol-MBP/Cu bicelles became stable against diluted and serum protein-containing conditions.

surfactant. For the construction of phospholipid bicelles that are stable under physiological environments, here we developed Chol-MBP (Fig. 1), a conjugate of cholic acid, the steroid backbone of CHAPSO, and a metal-binding peptide with an amino acid sequence of PHGGGPHGGG (MBP; Fig. 1), and we mixed Chol-MBP with 1,2-dipalmitoyl-*sn*-glycero-3-phosphorylcholine (DPPC, T_m = 41 °C)[5] that forms a kinetically stable gel-phase bilayer at a physiological temperature. PHGGG is a naturally occurring Cu^{2+}-binding motif that utilizes the metal-coordination ability of the imidazole groups in the histidine residues.[6] Namely, Chol-MBP is designed to self-assemble by the Cu^{2+}-mediated metal coordination. Upon mixing DPPC with Chol-MBP, phospholipid bicelles (DPPC/Chol-MBP bicelles) were formed, and subsequent incubation with Cu^{2+} to promote the self-assembly of Chol-MBP afforded crosslinked DPPC/Chol-MBP/Cu bicelles that showed increased stability against dilution and contamination of serum (Fig. 2).

We first synthesized the cholic acid-free MBP segment to investigate the Cu^{2+}-binding property and self-assembly. Upon titration with $CuCl_2$ (0.0–3.0 equivalents of Cu^{2+} to MBP) in water at 25 °C, MBP showed an increase in the absorption intensity around 580 nm in a stepwise manner until the addition of 2.0 equivalents of Cu^{2+}, and additional 1.0 equivalent of Cu^{2+} (3.0 equivalents in total) did not largely change the absorption spectrum (Fig. S1A in ESI†). The emerged absorption band is attributable to the *d-d* transition of Cu^{2+} complexed with MBP at its histidine residues.[7] Transmission electron microscopic (TEM) observation visualized the formation of micrometer-scale anisotropic aggregates after the addition of Cu^{2+} (Fig. 3B). Since aggregates of MBP were hardly observed in the absence of Cu^{2+} (Fig. 3A), it is likely that coordination between Cu^{2+} and histidine imidazole groups of multiple MBP molecules facilitates supramolecular polymerization into one-dimensional assemblies.

For the preparation of the bicelles consisting of DPPC and Chol-MBP, we mixed DPPC and Chol-MBP at the molar ratio of 4:1 (total content: 5.0 wt%) and performed the heating and cooling process between 25 and 60 °C for three times followed by 5-fold dilution (total content: 1.0 wt%), affording a

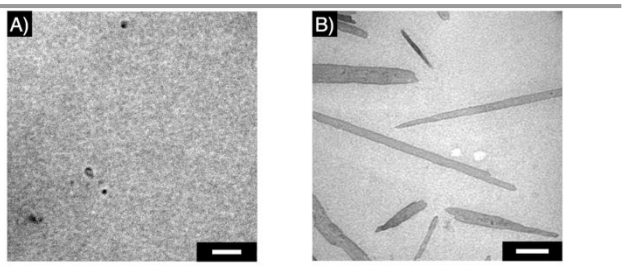

Fig. 3 TEM images of MBP (A) before and (B) after the addition of 2.0 equivalents of Cu^{2+} to MBP. Scale bar: 100 nm.

transparent dispersion (Fig. 4B). Bicelle formation was investigated by ^{31}P NMR analysis. The isotropic ^{31}P NMR peak at 0.0 ppm is observed in an isotropic state. It is known that the orientation of bicelles under the NMR magnetic field elicits a negative peak shift of the ^{31}P NMR signal from 0.0 ppm due to the chemical shift anisotropy of the ^{31}P atoms in the phospholipids.[8] Indeed, the mixture of DPPC and Chol-MBP showed a ^{31}P NMR signal at δ = –31.7 ppm at 25 °C, clearly indicating the formation of DPPC/Chol-MBP bicelles (Fig. 4D, upside). The broadening of the ^{31}P NMR signal as compared with conventional bicelles[8a] is likely due to the restricted motion of DPPC molecules in the gel-phase bilayer.[9] Interestingly, when CHAPSO was utilized instead of Chol-MBP for the preparation of bicelles at 1.0 wt%, the sample showed precipitation (Fig. 4A). Therefore, Chol-MBP likely stabilized the edge of the DPPC membranes more effectively than CHAPSO enabling the formation of bicelles under a diluted condition.

Upon addition of Cu^{2+} to DPPC/Chol-MBP bicelles ([Cu^{2+}]/[Chol-MBP] = 2/1), an absorption band at 580 nm derived from the Cu^{2+}-binding to the MBP segment emerged as observed in the case of MBP and Cu^{2+} complexation (Fig. S2 in ESI†). Importantly, even after the addition of Cu^{2+}, DPPC/Chol-MBP mixture was retained to be transparent (Fig. 4C) and its ^{31}P NMR spectral profile hardly changed (Fig. 4D, downside). These results indicate that the bicelle structure was essentially intact to the metal-binding process to form DPPC/Chol-MBP/Cu bicelles. Notably, the metal coordination with Cu^{2+} further enhanced the stability of DPPC/Chol-MBP bicelle. Upon additional 5-fold dilution of DPPC/Chol-MBP mixture (total content: 0.20 wt%), transmission electron micrographic (TEM) observation visualized spherical aggregates smaller than 100 nm in diameter (Fig. 4E). The sample showed a ^{31}P NMR signal at δ = 0.0 ppm (Fig. 4F).[10] Small-angle X-ray scattering (SAXS) measurement of the diluted mixture displayed a linear profile with a slope of –3 between *q* and scattering intensity in the small-*q* region, corresponding to the formation of aggregates with spherical morphologies (Fig. S3A in ESI†). These results indicate phase transition of DPPC/Chol-MBP bicelles into small size vesicles upon high dilution. In sharp contrast, DPPC/Chol-MBP/Cu mixture showed a negatively shifted ^{31}P NMR signal even at such a highly diluted condition ([Cu^{2+}]/[Chol-MBP] = 2/1, total content: 0.20 wt%, Fig. 4H). In SAXS measurement, a linear profile with a slope of –2 between *q* and scattering intensity was observed in the small-*q* region (Fig. S3B in ESI†), which is characteristic of disk-shaped colloids dispersed in water.[11] Consistently, TEM observation of DPPC/Chol-MBP/Cu mixture

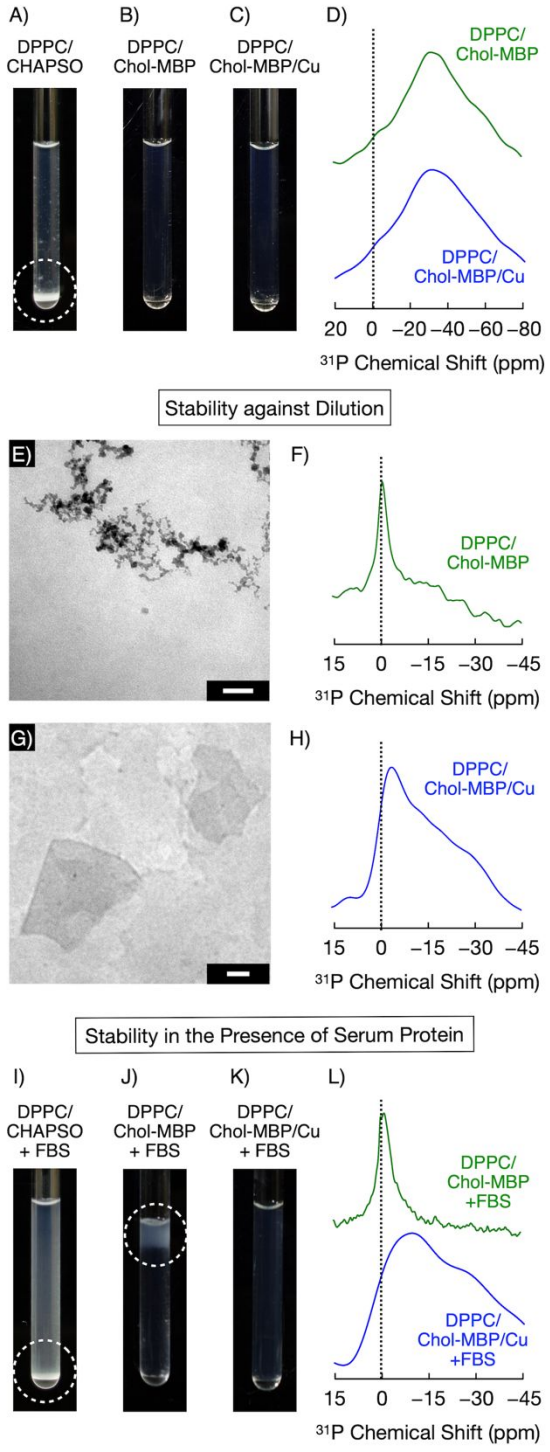

Fig. 4 Photographs of (A) the mixtures of DPPC and CHAPSO ([DPPC]/[Chol-MBP] = 4/1, 1.0 wt%), (B,C) DPPC and Chol-MBP ([DPPC]/[Chol-MBP] = 4/1, 1.0 wt%) (B) before and (C) after the addition of 2.0 equivalent of Cu^{2+} to Chol-MBP. The dashed circle in (A) indicates aggregation of the phospholipid assemblies. (D) ^{31}P NMR spectra of the mixtures of DPPC and Chol-MBP (upside) before and (downside) after the addition of Cu^{2+}. (E,G) TEM images of the mixtures of DPPC and Chol-MBP (total content = 0.20 wt%) (I) without and (K) with 2.0 equivalents of Cu^{2+}. Scale bars: 100 nm. (F,H) ^{31}P NMR spectra of the mixture of DPPC and Chol-MBP (total content = 0.20 wt%) (F) without and (H) with 2.0 equivalents of Cu^{2+} to Chol-MBP. Photographs of the mixtures of (I) DPPC and CHAPSO, and (J,K) DPPC and Chol-MBP (J) without and (K) with 2.0 equivalents of Cu^{2+} to Chol-MBP after incubation with FBS (1.0 wt%) at 25 °C for 18 h. (L) ^{31}P NMR spectra of the mixtures of DPPC and Chol-MBP (upside) without and (downside) with 2.0 equivalents of Cu^{2+} after the incubation with FBS (1.0 wt%) at 25 °C for 18 h.

showed two-dimensional disk structures (Fig. 4G). These results demonstrate that the metal coordination with Cu^{2+} significantly enhanced the stability of DPPC/Chol-MBP bicelles against the dilution process (Fig. 2).

As described in the introduction, considering *in vivo* applications of the bicelles, it is necessary that the disk structure is maintained under biological conditions such as in blood where serum proteins are contaminated and the concentration of the bicelles is diluted through blood circulation. When DPPC/Chol-MBP bicelles were incubated with fetal bovine serum (FBS, 1.0 wt%) for 18 h at 25 °C, white precipitates readily formed (Fig. 4J) as well as the case of DPPC/CHAPSO mixture (Fig. 4I). ^{31}P NMR analysis of DPPC/Chol-MBP mixture in the presence of FBS showed a relatively sharp signal at 0.0 ppm (Fig. 4L, upside), suggesting the formation of non-alignable isotropic aggregates. In contrast, the dispersion of DPPC/Chol-MBP/Cu bicelles at [Chol-MBP]/[Cu^{2+}] = 1/2 and 1/3 maintained the transparency (Fig. 4K) and showed a negatively shifted ^{31}P NMR signals (Fig. 4L, downside and Fig. S5 in ESI†) in the presence of FBS. Hence, self-assembly of Chol-MBP by the Cu^{2+} coordination was effective to stabilize the bicelle structure against not only the high dilution but also the contamination of serum proteins (Fig. 2), and we chose DPPC/Chol-MBP/Cu bicelles with [Chol-MBP]/[Cu^{2+}] = 1/2 as the adequate mixing ratio for the subsequent assays. We also confirmed that DPPC/Chol-MBP/Cu bicelle was maintained in the presence of glutathione at the concentration in blood[12] (30 μM, Fig. S6 in ESI†) and the cytotoxicity of DPPC/Chol-MBP/Cu bicelle was comparable to that of DPPC/CHAPSO mixture known to have low cytotoxicity[13] (Fig. S7 in ESI†).

Based on the characterization of DPPC/Chol-MBP/Cu bicelles indicating the enhanced stability against dilution and protein contamination, it was expected that DPPC/Chol-MBP/Cu bicelles would be a functional carrier for *in vivo* applications. We utilized DPPC/Chol-MBP/Cu bicelle for investigating the shape-dependency of phospholipid assemblies on the blood circulation profiles. As a proof-of-concept study, we prepared fluorescent DPPC vesicles and DPPC/Chol-MBP/Cu bicelles containing Cy5-labeled 1,2-dipalmitoyl-*sn*-glycero-3-phosphorylethanolamine (^{FL}DPPC vesicles and ^{FL}DPPC/Chol-MBP/Cu bicelles, respectively), and observed their blood circulation profiles by intravital confocal laser scanning microscopy (IV-CLSM)[14] at a mouse earlobe. Before the blood administration, both samples were filtered through membranes with 200 nm-pore to adjust the sizes. When ^{FL}DPPC vesicles were injected into mice via an artery (total content: 5.0 wt% before the injection), IV-CLSM showed that ^{FL}DPPC vesicles were aggregated and clogged (Fig. 5A). The time-course fluorescence profile indicated that ^{FL}DPPC vesicles were hardly transferred from the artery into the vein (Fig. 5B). In sharp contrast, ^{FL}DPPC/Chol-MBP/Cu bicelles (total content: 5.0 wt% before the injection) were homogeneously dispersed in the blood vessels (Fig. 5C) and the time-course fluorescence monitoring revealed prolonged circulation of ^{FL}DPPC/Chol-MBP/Cu bicelles (Fig. 5D). Hence, it was successfully demonstrated that phospholipid bicelles show prolonged circulation in the blood vessel relative to the spherical vesicles.

Therefore, it is likely that the stabilized phospholipid bicelles could be a suitable carrier to the whole body by blood administration.

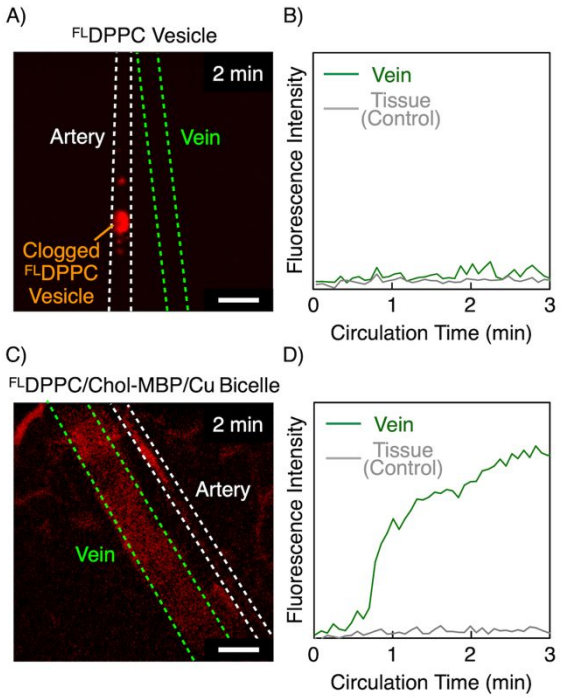

Fig. 5 IV-CLSM images (λ_{ext} = 640 nm) of blood vessels at mouse earlobe 2 min after the injection of (A) ^{FL}DPPC vesicles (total content: 5.0 wt% before the injection) and (C) ^{FL}DPPC/Chol-MBP/Cu bicelles (total content: 5.0 wt% before the injection). Scale bars: 100 μm. Time-course profiles of fluorescence intensities of (B) ^{FL}DPPC vesicles and (D) ^{FL}DPPC/Chol-MBP/Cu bicelles. The fluorescence was monitored in a vein (green) and a tissue (gray) as a control.

In this work, we have reported phospholipid-based DPPC/Chol-MBP/Cu bicelles prepared by mixing Chol-MBP and DPPC and subsequent metal coordination with Cu^{2+}. DPPC/Chol-MBP/Cu bicelles maintained the disk shape against high dilution and contamination of serum proteins and showed an extended blood circulation property compared with spherical DPPC vesicles, suggesting a potential utility for drug delivery systems in blood administration. Such a stabilized bicelle could be also useful as membrane mimetics for structural and biochemical studies of membrane proteins,[3a] microbial peptides,[3b] and amyloid peptides[3c] in diluted and contaminated conditions.

This work was supported by JST CREST JPMJCR19S4 (TM), the Mazda Foundation (TM), KAKENHI JP21H05096 (TM) and JP19K15378 (NU), JACI (NU), and Moritani Foundation (NU). SAXS measurements were performed at Open Facility Center at Tokyo Institute of Technology.

Conflicts of interest

The authors declare no competing interests.

Notes and references

1 a) A. Sharma and U. S. Sharma, *Int. J. Pharm.*, 1997, **154**, 123; b) G. Bozzuto and A. Molinari, *Int. J. Nanomed.*, 2015, **10**, 975; c) W. J. Mulder, G. J. Strijkers, G. A. van Tilborg, D. P. Cormode, Z. A. Fayad and K. Nicolay, *Acc. Chem. Res.*, 2009, **42**, 904.

2 a) R. V. Mannige, T. K. Haxton, C. Proulx, E. J. Robertson, A. Battigelli, G. L. Butterfoss, R. N. Zuckermann and S. Whitelam, *Nature*, 2015, **526**, 415; b) R. Kurapati, K. Kostarelos, M. Prato and A. Bianco, *Adv. Mater.*, 2016, **28**, 6052; c) Y. Suzuki, G. Cardone, D. Restrepo, P. D. Zavattieri, T. S. Baker and F. A. Tezcan, *Nature*, 2016, **533**, 369; d) D. H. N. Dürr, M. Gildenberg and A. Ramamoorthy, *Chem. Rev.*, 2012, **112**, 6054; e) I. Marcotte and M. Auger, *Concepts Magn. Reson. Part A*, 2005, **24A**, 17; f) C. R. Sanders and R. S. Prosser, *Structure*, 1998, **6**, 1227; g) R. R. Vold, R. S. Prosser and A. J. Deese, *J. Biomol. NMR*, 1997, **9**, 329; h) L. Barbosa-Barros, G. Rodríguez, C. Barba, M. Cócera, L. Rubio, J. Estelrich, C. López-Iglesias, A. de la Maza and O. López, *Small*, 2012, **8**, 807; i) S. Muro, C. Garnacho, J. A. Champion, J. Leferovich, C. Gajewski, E. H. Schuchman, S. Mitragotri and V. R. Muzykantov, *Mol. Ther.*, 2008, **16**, 1450; j) N. Doshi, B. Prabhakarpandian, A. Rea-Ramsey, K. Pant, S. Sundaram and S. Mitragotri, *J. Controlled Release*, 2010, **146**, 196; k) G. Adriani, M. D. de Tullio, M. Ferrari, F. Hussain, G. Pascazio, X. Liu and P. Decuzzi, *Biomaterials*, 2012, **33**, 5504; l) L. Lin, X. Liang, Y. Xu, Y. Yang, X. Li and Z. Dai, *Bioconjugate Chem.*, 2017, **28**, 2410; m) L. Lin, X. Wang, Y. Guo, K. Ren, X. Li, L. Jing, X. Yue, Q. Zhang and Z. Dai, *RSC Adv.*, 2016, **6**, 79811; n) K. Yasuhara, S. Miki, H. Nakazono, A. Ohta and J. Kikuchi, *Chem. Commun.*, 2011, **47**, 4691; o) S. N. Tenjarla, J. H. Holbrook, P. Puranajoti, C. Pegc, K. D. Lowe, T. E. Jackson and A. Smith, *J. Toxicol. Cut & Ocular Toxicol.*, 1995, **14**, 299.

3 a) B. Krishnarjuna, T. Ravula, A. Ramamoorthy, *Chem. Commun.*, 2020, **56**, 6511; b) B. R. Sahoo, T. Genjo, S. J. Cox, A. K. Stoddard, G.M. Anantharamaiah, C. Fierke, A. Ramamoorthy, *J. Mol. Biol.,* 2018, **430**, 4230; c) T.-J. Park, J.-S. Kim, H.-C. Ahn and Y. Kim, *Biophys. J.,* 2011, **101**, 1193; d) N. Z. Hardin, V. Kocman, G. M. Di Mauro, T. Ravula, A. Ramamoorthy, *Angew. Chem. Int. Ed.,* 2019, **58**, 17246.

4 K. Shimizu, Y. Maitani, K. Takayamai and T. Nagai, *Biol. Pharm. Bull.*, 1997, **20**, 811.

5 K. S. Mineev, K. D. Nadezhdin, S. A. Goncharuk and A. S. Arseniev, *Langmuir*, 2016, **32**, 6624.

6 S. Ghosh and S. Verma, *Tetrahedron Lett.*, 2007, **48**, 2189.

7 A. I. Banerjee, L. Yu and H. Matsui, *Proc. Natl. Acad. Sci.*, 2003, **100**, 14678.

8 a) F. Picard, M. Paquet, J. Lévesque, A. Bélanger and M. Auger, *Biophys. J.*, 1999, **77**, 888; b) G. Raffard, S. Steinbruckner, A. Arnold, J. H. Davis and E. J. Dufourc, *Langmuir*, 2000, **16**, 7655.

9 R. Bärenwald, A. Achilles, F. Lange, T. M. Ferreira, K. Saalwächter, *Polymer*, 2016, **8**, 439.

10 M. Traïkia, D. E. Warschawski, M. Recouvreur, J. Cartaud, P. F. Devaux, *Eur. Biophys. J.,* 2000, **29**, 184.

11 D. Yamaguchi, N. Miyamoto, S. Koizumi, T. Nakato and Hashimoto, T. *Appl. Cryst.*, 2007, **40**, s101.

12 A. Pastore, F. Piemonte, M. Locatelli, A. L. Russo, L. M. Gaeta, G. Tozzi and G. Federici, *Clin. Chem.,* 2021, **47**, 1467.

13 L. Vian, J. Vincent, J. Maurin, I. Fabre, J. Giroux and J. P. Cano, *Toxic. in Vitro,* 2000, **29**, 184.

14 A. Tao, G. L. Huang, K. Igarashi, T. Hong, S. Liao, F. Stellacci, Y. Matsumoto, T. Yamasoba, K. Kataoka and H. Cabral, *Macromol. Biosci.*, 2020, **20**, 1900161.